Reduced tubulin polyglutamylation suppresses flagellar shortness in *Chlamydomonas*

Tomohiro Kubo[a,b], Masafumi Hirono[b], Takumi Aikawa[b], Ritsu Kamiya[b,c], and George B. Witman[a]
[a]Department of Cell and Developmental Biology, University of Massachusetts Medical School, Worcester, MA 01655;
[b]Department of Biological Sciences, Graduate School of Science, University of Tokyo, Tokyo 113-0033, Japan;
[c]Department of Life Science, Faculty of Science, Gakushuin University, Tokyo 171-8588, Japan

ABSTRACT **Ciliary length control is an incompletely understood process essential for normal ciliary function. The flagella of *Chlamydomonas* mutants lacking multiple axonemal dyneins are shorter than normal; previously it was shown that this shortness can be suppressed by the mutation *suppressor of shortness 1* (*ssh1*) via an unknown mechanism. To elucidate this mechanism, we carried out genetic analysis of *ssh1* and found that it is a new allele of *TPG2* (hereafter *tpg2-3*), which encodes FAP234 functioning in tubulin polyglutamylation in the axoneme. Similar to the polyglutamylation-deficient mutants *tpg1* and *tpg2-1*, *tpg2-3* axonemal tubulin has a greatly reduced level of long polyglutamate side chains. We found that *tpg1* and *tpg2-1* mutations also promote flagellar elongation in short-flagella mutants, consistent with a polyglutamylation-dependent mechanism of suppression. Double mutants of *tpg1* or *tpg2-1* and *fla10-1*, a temperature-sensitive mutant of intraflagellar transport, underwent slower flagellar shortening than *fla10-1* at restrictive temperatures, indicating that the rate of tubulin disassembly is decreased in the polyglutamylation-deficient flagella. Moreover, α-tubulin incorporation into the flagellar tips in temporary dikaryons was retarded in polyglutamylation-deficient flagella. These results show that polyglutamylation deficiency stabilizes axonemal microtubules, decelerating axonemal disassembly at the flagellar tip and shifting the axonemal assembly/disassembly balance toward assembly.**

Monitoring Editor
Wallace Marshall
University of California, San Francisco

Received: Apr 1, 2015
Revised: Jun 8, 2015
Accepted: Jun 8, 2015

INTRODUCTION

Eukaryotic cilia and flagella (here used as interchangeable terms) comprise >600 proteins (Pazour *et al.*, 2005), the majority of which are assembled into the well-ordered "9 + 2" axonemal structure. A major challenge has been to clarify the molecular mechanism underlying the establishment of exact length of cilia. Although much progress has been made (Ishikawa and Marshall, 2011), important questions remain unanswered.

Assembly of cilia relies on intraflagellar transport (IFT), a bidirectional transport system in which the motor proteins kinesin-2 and cytoplasmic dynein 1b/2 drive the movement of trains of IFT particles along the axonemal microtubules. First reported in *Chlamydomonas* flagella (Kozminski *et al.*, 1993), IFT is known to play a critical role in the assembly of almost all kinds of cilia. In both growing and steady-state flagella, IFT trains are constantly moving in and out of the organelle to transport various cargoes of axonemal components, which include tubulin (Marshall and Rosenbaum, 2001), radial spoke proteins (Qin *et al.*, 2004), dynein arm proteins (Piperno *et al.*, 1996; Hou *et al.*, 2007), and nexin-dynein regulatory complex (N-DRC) proteins (Wren *et al.*, 2013). Loss of IFT-particle proteins or the IFT motors in *Chlamydomonas* results in short, stumpy flagella or sometimes complete loss of flagella (Pazour *et al.*, 1999, 2000; Porter *et al.*, 1999; Deane *et al.*, 2001; Hou *et al.*, 2007). Temporary inhibition of IFT in *fla10-1*, a temperature-sensitive mutant carrying a mutation in the anterograde motor kinesin-2, causes gradual flagellar shortening that reflects the axoneme disassembly rate in the steady state of wild-type cells (Kozminski *et al.*, 1995). The balance between the rates of assembly and disassembly of axonemes, determined by the rates of incorporation and dissociation of tubulin and other axonemal proteins, is believed to be an important determinant of flagellar length (Marshall and Rosenbaum, 2001).

This article was published online ahead of print in MBoC in Press (http://www.molbiolcell.org/cgi/doi/10.1091/mbc.E15-03-0182) on June 17, 2015.

Address correspondence to: George B. Witman (george.witman@umassmed.edu)

Abbreviations used: AFLP, amplified-fragment-length polymorphism; DIC, differential interference contrast; IFT, intraflagellar transport; NaPPi, sodium pyrophosphate; N-DRC, nexin-dynein regulatory complex.

Besides IFT, other factors also are known to be crucial for producing flagella of proper length. These factors include a variety of protein kinases (Berman *et al.*, 2003; Wilson and Lefebvre, 2004; Bradley and Quarmby, 2005; Tam *et al.*, 2007, 2013; Hilton *et al.*, 2013) and microtubule-depolymerizing kinesins (Cao *et al.*, 2009). For example, kinesin-13 controls flagellar length by regulating the amount of free tubulin derived from the cytoplasmic pool (Piao *et al.*, 2009; Wang *et al.*, 2013), whereas another kinesin, KIF-19A, localized at the ciliary tip, promotes the depolymerization of the axonemal microtubules to maintain normal ciliary length (Niwa *et al.*, 2012).

In addition to these factors that may be specifically involved in flagellar length determination, the presence or absence of a variety of axonemal structures, which include inner and outer dynein arms, radial spokes, and the central pair of microtubules, is known to affect flagellar length. In particular, *Chlamydomonas* mutants lacking multiple axonemal dynein species often display defects in flagellar length control (Huang *et al.*, 1979; LeDizet and Piperno, 1995). For example, the mutant *pf13*, lacking outer arm dynein and inner arm dynein c in the axoneme (Omran *et al.*, 2008; Yamamoto *et al.*, 2010), has short flagella (Huang *et al.*, 1979). Similarly, the *pf23* mutant, lacking inner arm dyneins a, c, d, and f/I1, also has short flagella (Huang *et al.*, 1979; Supplemental Figure S1, A and D). The double mutant of *pf28* (an *ODA2* allele resulting in loss of outer arm dynein; Mitchell and Rosenbaum, 1985; Kamiya, 1988) and *pf30* (an *IDA1* allele causing loss of inner arm dynein f/I1; Brokaw and Kamiya, 1987; Kamiya *et al.*, 1991) almost completely fails to assemble flagella under normal conditions. The mechanism by which the presence or absence of these dyneins influences flagellar length is not known.

Previously, a mutant that suppresses the flagellar shortness of *pf28pf30* was isolated and designated *ssh1* for *suppressor of shortness 1* (Gianni Piperno, personal communication; LeDizet and Piperno, 1995). The triple mutant *pf28pf30ssh1* (also called the WS4 strain; Freshour *et al.*, 2007) displays flagella of normal length, although they still lack outer arm dynein and inner arm dynein f/I1. This phenotype of *pf28pf30ssh1* has enabled researchers to explore biochemical and physiological properties of flagella lacking these two dyneins (LeDizet and Piperno, 1995; Freshour *et al.*, 2007; Tanner *et al.*, 2008; Wirschell *et al.*, 2008, 2009). However, the identity of the *ssh1* mutation and the mechanism by which it restores flagellar length have not been determined.

In this study, we found that the gene mutated in *ssh1* is *TPG2*, a gene encoding FAP234 (Kubo *et al.*, 2014), which is a protein that forms a complex with the polyglutamylase TTLL9/FAP267 (Kubo *et al.*, 2010) and is essential for normal addition of long polyglutamate side chains to α-tubulin in the axoneme, predominantly on the B-tubule of the outer doublets (Lechtreck and Geimer, 2000; Kubo *et al.*, 2010). Previous studies showed that tubulin polyglutamylation is important for the stability (Pathak *et al.*, 2007) and motility of cilia/flagella (Kubo *et al.*, 2010; Suryavanshi *et al.*, 2010). The present study revealed an additional function of tubulin polyglutamylation: flagellar length control through modulation of the kinetics of axoneme assembly/disassembly.

RESULTS

ssh1 lacks the TTLL9-FAP234 complex and has greatly reduced polyglutamylated tubulin in the axoneme

The *ssh1* mutation in a wild-type background causes slightly reduced beat frequency and swimming velocity (Freshour *et al.*, 2007; Figure 1A) but results in complete loss of motility when combined with *pf28* or *oda2* mutations, which cause loss of outer arm dynein (Freshour *et al.*, 2007; unpublished data). This suggests that *ssh1* has a defect in some inner arm dynein function, because the combined loss of outer arm dynein and some inner arm dyneins is known to cause complete loss of motility (Kamiya, 2002). However, *ssh1* axonemes have an apparently normal composition of axonemal dyneins (T.K., unpublished data). This phenotype is reminiscent of those of the mutants *tpg1*, *tpg2-1*, and *tpg2-2*. *TPG1* encodes TTLL9, a polyglutamylating enzyme, whereas *TPG2* encodes FAP234, a TTLL9-associated protein (Kubo *et al.*, 2010, 2014); these two proteins form a complex that is present in both the flagellar axoneme and membrane-plus-matrix fractions. *tpg1* lacks TTLL9, whereas the *tpg2* mutants lack FAP234 and also TTLL9, which requires FAP234 for its stability. All three mutants display a lowered level of axonemal tubulin polyglutamylation due to the absence of TTLL9.

To determine whether TTLL9 or FAP234 levels were affected in *ssh1*, we analyzed isolated axonemes of *ssh1* and wild-type cells by Western blotting. The results indicated that *ssh1* axonemes lack both proteins, as do the axonemes of *tpg1* and *tpg2-1* (Figure 1B). As reported (Kubo *et al.*, 2010), antibody polyE, specific for polyglutamate side chains of three or more residues, strongly detected tubulin in wild-type axonemes (Figure 1B); no other polyglutamylated proteins were detected in the axoneme, even after extended exposure times (Supplemental Figure S2A). Tubulin also was strongly detected in wild-type axonemes by the antibody B3, which is specific for polyglutamylated tubulin (Figure 1, B and D, and Supplemental Figure S2B). Tubulin polyglutamylation detected by both antibodies was greatly reduced in *ssh1*, as in *tpg1* and *tpg2-1* (Figure 1B and Supplemental Figure S2). This tubulin polyglutamylation deficiency would explain the complete loss of flagellar motility in *ssh1* and *pf28* or *oda2* double mutants, because tubulin polyglutamylation is known to be important for the function of inner arm dynein e (Kubo *et al.*, 2012).

ssh1 has a mutation in the gene encoding FAP234

The lack of the TTLL9-FAP234 complex in the *ssh1* axoneme raised the possibility that *ssh1* is an allele of *TPG1* or *TPG2*. Amplified-fragment-length polymorphism (AFLP) analysis located the *ssh1* mutation to linkage group I, where *TPG2* (*FAP234*) has been mapped (Kubo *et al.*, 2014). Sequencing of the *TPG2* cDNA from *ssh1* detected a 16–base pair insertion (GCCTCCGCCGCGGCCG) in exon 26 (Figure 1C). Thus *ssh1* is an allele of *TPG2*. Because two mutant alleles of *TPG2* already have been described, this allele will hereafter be designated *tpg2-3*. The insertion in this mutant was predicted to cause a frameshift and a premature stop codon at exon 28. Because Western blotting using both anti-FAP234N antibody (T.K., unpublished data) and anti-FAP234C antibody (Figure 1, B and D) failed to detect any full-length or truncated FAP234 in the *tpg2-3* axoneme, most transcripts likely are degraded in the cytoplasm.

Tubulin polyglutamylation deficiency promotes flagellar growth in mutants lacking various axonemal components

From the finding that *ssh1* is an allele of *TPG2*, we surmised that the great reduction in axonemal tubulin polyglutamylation resulting from loss of the TTLL9/FAP234 complex might suppress flagellar shortness. Because we had not examined this hypothesis using *tpg1* or *tpg2* mutations previously, we measured flagellar length in various mutants with and without the *tpg1*or *tpg2* mutations. First, we found that the flagellar length in *tpg1*, *tpg2-1*, and *tpg2-3* cells is slightly longer than in wild type (Figure 2Aa). Kubo *et al.* (2010) reported that the flagellar length of *tpg1* is the same as that of wild type; this discrepancy is most likely due to the difference in

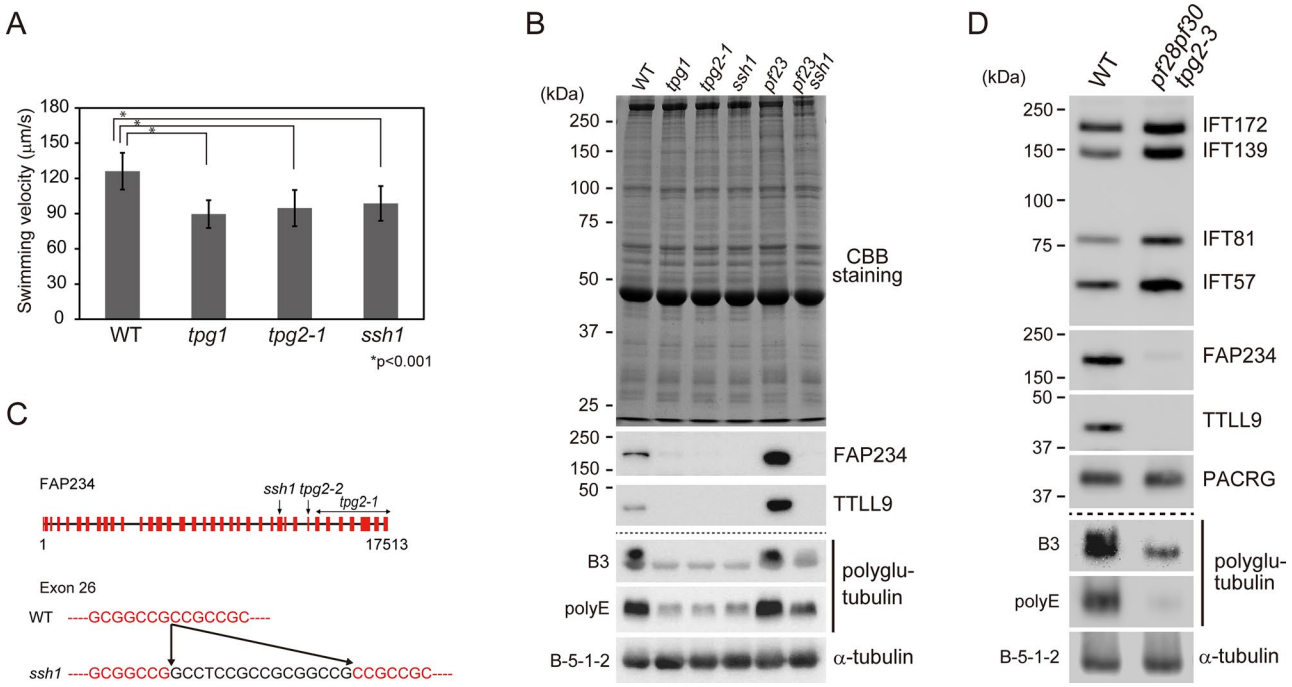

FIGURE 1: *ssh1* is an allele of *TPG2*, which encodes FAP234, a flagella-associated protein involved in axonemal tubulin polyglutamylation. (A) Swimming velocities of wild type (WT), *tpg1*, *tpg2-1*, and *ssh1*. At least 20 cells were measured to obtain the average velocities. SDs for each measurement are shown as bars. Asterisks indicate statistically significant differences (*t* test, $p < 0.001$). (B) Western blot analysis of axonemes of WT, *tpg1*, *tpg2-1*, *ssh1*, *pf23*, and *pf23ssh1*. SDS–polyacrylamide gels were either stained with Coomassie brilliant blue or blotted with antibodies that recognize FAP234, TTLL9, polyglutamylated tubulin (B3 antibody), polyglutamate side chains (polyE antibody), and α-tubulin (B-5-1-2). (C) Schematic illustration of genomic sequence encoding FAP234 with the mutation sites of *tpg2-1*, *tpg2-2*, and *ssh1* (top). Partial sequences of exon 26 are shown (red, bottom). *ssh1* has a 16–base pair insertion in exon 26 (black). (D) Western blot analysis of isolated flagella of WT and *pf28pf30tpg2-3* probed with the indicated antibodies. *pf28pf30tpg2-3* has increased amounts of IFT-particle proteins.

the culture media used: the present study used liquid minimal (M) medium, containing no acetate, whereas the previous studies used standard Tris-acetate-phosphate (TAP) medium, containing acetate, which can inhibit flagellar growth in some mutants (Jarvik *et al.*, 1984). Indeed, the remeasurement of flagellar length in TAP medium confirmed that *tpg1* and *tpg2-1* have flagellar lengths similar to that of wild type under those growth conditions (Supplemental Figure S3A).

We then examined the effect of the *tpg1* and *tpg2* mutations on the flagellar length of the mutant *pf23* as well as the double mutant *pf28pf30*, in which the effect of the *ssh1* mutation was first identified (Gianni Piperno, personal communication). Like *pf28pf30* (lacking inner arm f/I1 and outer arm dynein), *pf23* (lacking inner arm dyneins a, c, d, and f/I1) has difficulty assembling flagella (Figure 2, B, a and b, and C, and Supplemental Figure S1, A and D); cells mostly lack flagella but produce short flagella after treatment with autolysin, a cell-wall-digesting enzyme (Figure 2Bc and Supplemental Figure S1, C and D). However, double mutants *pf23tpg1*, *pf23tpg2-1*, and *pf23tpg2-3* and triple mutants *pf28pf30tpg1*, *pf28pf30tpg2-1*, and *pf28pf30tpg2-3* produced flagella that are significantly longer than *pf23* and *pf28pf30* flagella possessing normal levels of tubulin polyglutamylation (Figure 2, A, a and b, B, a–d, and C, and Supplemental Figure S1, B and D). The fact that mutant alleles of either *TPG1* or *TPG2*, both of which are needed for normal tubulin polyglutamylation, suppress flagellar shortness in mutants lacking multiple dyneins indicates that this suppression is likely due to reduction in axonemal tubulin polyglutamylation caused by loss of TTLL9.

To determine whether the loss of the TTLL9/FAP234 complex suppresses flagellar shortness associated with other types of axonemal defects, we examined another double mutant, *oda3ida1*, which lacks the outer dynein arm docking complex (Takada and Kamiya, 1994; Koutoulis *et al.*, 1997), as well as inner arm dynein f/I1. Cells of *oda3ida1* lack flagella under normal conditions and have flagella much shorter than wild-type cells after treatment with autolysin (Figure 2, Ab and C). However, *tpg2-1* restores full flagellar length to *oda3ida1*, even in the absence of autolysin treatment. We also examined the effect on cells lacking the N-DRC, a multisubunit complex that regulates the dyneins and constitutes the nexin link that cross-bridges adjacent outer doublets (Piperno *et al.*, 1992; Heuser *et al.*, 2009). N-DRC–deficient mutants such as *pf2*, *pf3*, and *ida6* display shorter flagella (Piperno *et al.*, 1992; Kato *et al.*, 1993); the flagella become still shorter when these mutants are combined with a mutation lacking either outer or inner arm dyneins (Piperno *et al.*, 1992; Kato *et al.*, 1993). We tested one such double mutant, *ida4pf3*, which lacks several N-DRC subunits as well as several inner arm dyneins, and found that when it was combined with *tpg1*, both the number of cells with flagella and flagellar length were greatly increased (Figure 2, Ac, B, e and f, and C). Finally, we compared flagella lengths in several single mutants lacking dynein(s) and non-dynein axonemal components with or without the *tpg1* or *tpg2-1* mutation. Mutants lacking inner arm dynein(s), outer arm dynein, the central pair complex, and radial spokes all exhibited slightly longer flagella when they were combined with either *tpg* mutation (Supplemental Figure S3, B–D). These results show that loss of the

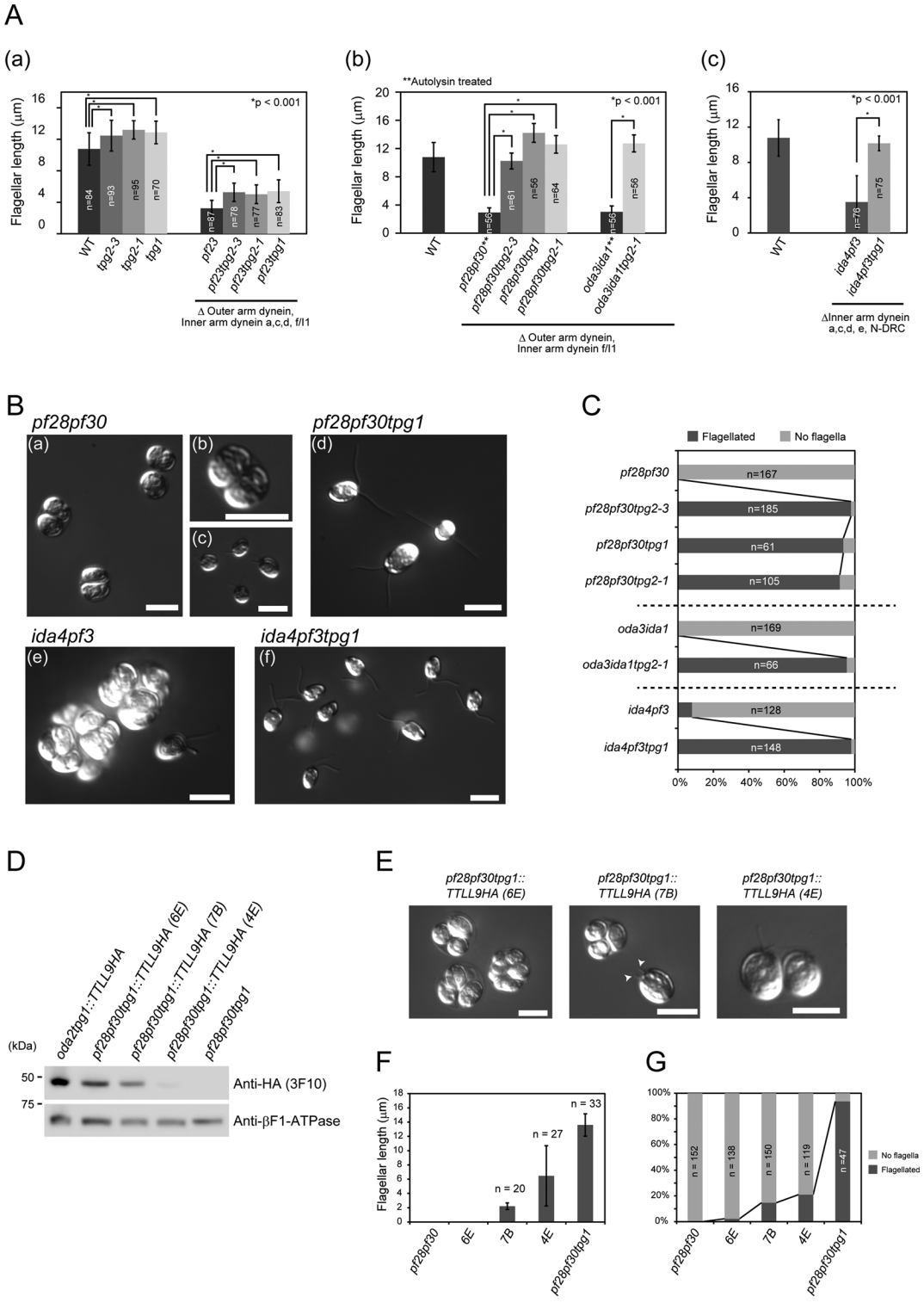

FIGURE 2: *tpg2-1* and *tpg1* mutations increase the flagellar growth in mutants lacking multiple components of the axoneme. (A) (a) Flagellar length in WT, *tpg2-3*, *tpg2-1*, *tpg1*, *pf23*, *pf23tpg2-3*, *pf23tpg2-1*, and *pf23tpg1*. (b) Flagellar length in *pf28pf30* (autolysin treated), *pf28pf30tpg2-3*, *pf28pf30tpg1*, *pf28pf30tpg2-1*, *oda3ida1* (autolysin treated), and *oda3ida1tpg2-1*. (c) Flagellar length in WT, *ida4pf3*, and *ida4pf3tpg1*. SDs for each measurement are shown as bars. Asterisks indicate statistically significant differences (*t* test, $p < 0.001$). (B) (a–c) *pf28pf30*, (d) *pf28pf30tpg1*, (e) *ida4pf3*, and (f) *ida4pf3tpg1* observed by DIC microscopy. In c, *pf28pf30* cells were treated with autolysin. (C) Ratio of flagellated cells under normal conditions (no autolysin treatment). (D) Western blot of whole cells of the indicated strains probed with anti–HA-tag (3F10) and anti–βF1-ATPase antibodies (loading control). (E) Three different *pf28pf30tpg1::TTLL9HA* transformants (6E, 7B, and 4E) observed by DIC microscopy. The arrowheads in the middle image indicate stumpy flagella. Flagellar length (F) and presence or absence of flagella (G) in *pf28pf30tpg1::TTLL9HA* transformants and controls. All of the strains presented here were cultured in M medium.

TTLL9/FAP234 complex is generally effective in suppressing flagellar shortness associated with axonemal structural deficiencies. Although our experiments do not exclude the possibility that the TTLL9/FAP234 complex is functioning nonenzymatically, it seems most likely that the suppression is due to the decrease in tubulin polyglutamylation that accompanies loss of these proteins.

Reversal of suppression of flagellar shortness by transformation with the *TPG1* gene

To examine further the role of tubulin polyglutamylation in flagellar length control, we cotransformed the triple mutant *pf28pf30tpg1*, which lacks the polyglutamylating enzyme TTLL9 and displays normal-length flagella, with a genomic DNA fragment encoding the TTLL9 sequence fused to a hemagglutinin (HA) tag together with a paromomycin-resistant gene. We recovered 288 paromomycin-resistant transformants; of these, 15 clones had clumpy (i.e., palmelloid) phenotypes indicative of an inability to properly assemble flagella. Western blotting of whole-cell lysates of three different transformants displaying palmelloid phenotypes revealed that all three expressed TTLL9-HA (Figure 2D). Of importance, the level of TTLL9-HA expression correlated inversely with the ability to form flagella and with flagellar length (Figure 2, D–G). These results provide additional strong support for the hypothesis that flagellar length in dynein-deficient mutants is dependent on the level of tubulin polyglutamylation.

Tubulin polyglutamylation deficiency does not affect IFT

Because the negative charge of the polyglutamate side chain in the tubulin C-terminal region could affect the functions of microtubule motors (Okada and Hirokawa, 2000; Sirajuddin *et al.*, 2014), tubulin polyglutamylation deficiency might well change IFT dynamics and thereby promote flagellar elongation. To address this hypothesis, we examined the amount, velocities, and frequencies of IFT particles in *Chlamydomonas tpg1* and *tpg2-1* flagella.

Western blotting showed that *tpg1* and *tpg2-1* flagella have nearly normal amounts of IFT-particle proteins (IFT172, IFT139, IFT81, and IFT57) and dynein 1b subunits (Dhc1b and D1bLIC; Figure 3A). In addition, indirect immunofluorescence microscopy showed normal distribution of IFT46 along the flagella (Figure 3B), and differential interference contrast (DIC) microscopy indicated normal speeds and frequencies of IFT-particle proteins in *tpg1* and *tpg2-1* flagella (Figure 3, C–E). The absence of a detectable effect of polyglutamylation deficiency on IFT suggests that the deficiency increases flagellar length through an IFT-independent mechanism. O'Hagan *et al*. (2011) showed that, in *Caenorhabditis elegans* sensory cilia, an increase in tubulin polyglutamylation caused by loss of the tubulin deglutamylase CCPP-1 increased the velocity of the IFT accessory motor OSM-3 but not that of heterotrimeric kinesin-2, the canonical anterograde IFT motor. Because *Chlamydomonas* anterograde IFT is driven only by kinesin-2, our results are consistent with those of O'Hagan *et al*. (2011).

Tubulin polyglutamylation deficiency inhibits flagellar shortening of *fla10-1* at restrictive temperatures

The mutant *fla10-1* has a temperature-sensitive mutation in the gene encoding FLA10, one of the heavy chains of the anterograde IFT motor kinesin-2. This mutant has normal-length flagella at permissive temperature (23°C), but a shift to restrictive temperature (33°C) induces gradual shortening of its flagella (Kozminski *et al.*, 1995). The shortening speed of *fla10-1* flagella at the restrictive temperature is believed to reflect the disassembly rate of wild-type axonemes at steady state. Therefore, to evaluate the effect of tubulin polyglutamylation deficiency on axonemal disassembly, we examined the kinetics of temperature-induced flagellar shortening of a double mutant of *fla10-1* combined with *tpg1* or *tpg2-1*. The double mutants had flagellar lengths similar to those of *fla10-1* at the permissive temperature, but their flagella shortened at only 21% (*fla10tpg1*) or 16% (*fla10tpg2-1*) of the rate of the *fla10-1* flagella after the shift to the restrictive temperature (Figure 4A, a and b). The amounts of IFT-particle proteins IFT172, IFT139, IFT81, and IFT57 in the flagella of *fla10-1* as well as *fla10tpg2-1* greatly decreased after the temperature shift, confirming that IFT was inhibited in these flagella (Figure 4Ac). These results suggest that the tubulin polyglutamylation deficiency decreases the steady-state rate of axonemal disassembly, thus slowing the temperature-induced flagellar shortening of *fla10-1*.

Tubulin polyglutamylation deficiency inhibits premeiotic flagellar shortening

The mating of *Chlamydomonas* plus and minus mating-type gametes results in the formation of a quadriflagellated dikaryon. Sometime after the dikaryon has formed, its flagella will undergo two phases of synchronized shortening: 1) a gradual shortening phase lasting 2–3 h, followed by 2) a rapid, catastrophic shortening phase lasting ~30 min and resulting in complete resorption of the flagella (Cavalier-Smith, 1974; Marshall and Rosenbaum, 2001; Pan and Snell, 2005). To investigate whether tubulin polyglutamylation affects this premeiotic flagellar shortening, we produced dikaryons between CC124 and CC125 (wild-type dikaryon), *tpg1* and *tpg1*, *tpg2-1* and *tpg2-1,* and *tpg1* and *tpg2-1*. The frequency of dikaryon formation in all crosses was normal (T.K., unpublished data), indicating that the *tpg* mutations do not affect mating kinetics. We then measured the average length of flagella in the populations of zygotes. As expected, the average flagellar length of wild-type dikaryons gradually decreased after mating (Figure 4Ba). Strikingly, the dikaryons between *tpg1* and *tpg1* or between *tpg2-1* and *tpg2-1* did not show flagellar shortening within 4 h (Figure 4B), indicating a very slow rate of axonemal disassembly in the polyglutamylation-deficient dikaryons.

A potential concern was that if our data included cells undergoing catastrophic shortening and if this was initiated earlier in wild-type dikaryons than in mutant dikaryons, it might give an erroneous impression of more rapid shortening in the wild-type population. However, this was not the case. First, our data excluded all dikaryons lacking flagella, so cells having completed catastrophic shortening would not have been included. Second, the distribution of flagellar lengths in the CC124 × CC125 dikaryons showed a fairly sharp peak that over time moved toward shorter length (Supplemental Figure S4). If occasional cells undergoing catastrophic shortening had been included, these would have been revealed as outliers having shorter flagella. Therefore it is likely that nearly all cells included in the data set were undergoing the first, slow phase of premeiotic flagellar shortening. The mutant dikaryons had a similarly narrow distribution of flagellar lengths, but in these populations, the peak moved toward shorter lengths much more slowly (Supplemental Figure S4).

In the heterologous *tpg1* × *tpg2-1* dikaryons, there was a lag (~1 h), followed by flagellar shortening at near-normal rate (Figure 4B). This undoubtedly reflects temporary dikaryon rescue (a process in which a protein supplied by one of the gametes can rescue a deficiency of its mating partner). Although our previous data showed that temporary dikaryon rescue (recovery of tubulin polyglutamylation) did not occur in *tpg1* × *tpg2-1* heterodikaryons within 60 min of mating (Kubo *et al.*, 2014), the longer incubation after initiation of the mating reaction in the present study likely allowed the heterodikaryons to recover the axonemal tubulin polyglutamylation

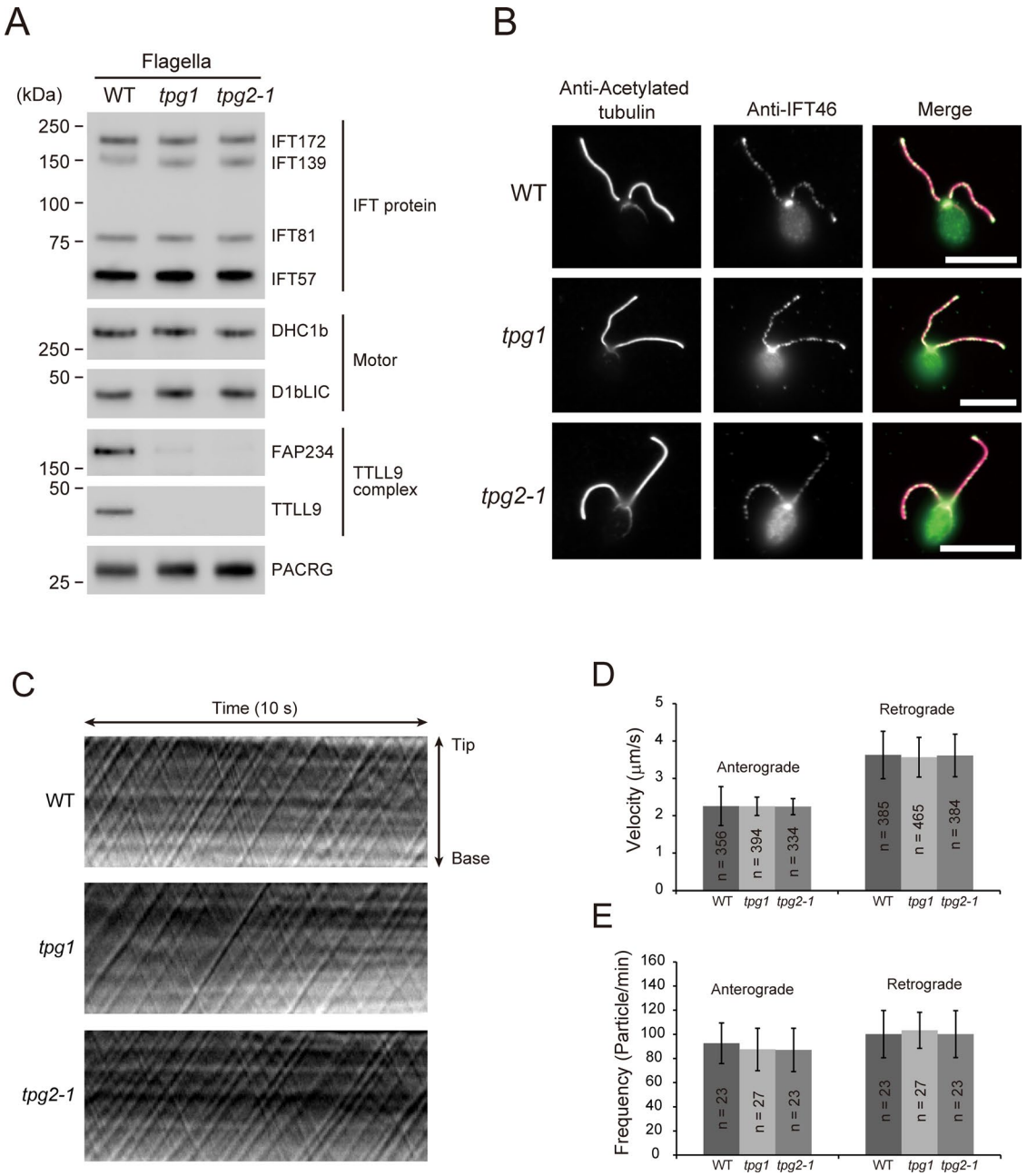

FIGURE 3: *tpg1* and *tpg2-1* have normal IFT. (A) Western blot of isolated flagella of WT, *tpg1*, and *tpg2-1* probed with antibodies to proteins as indicated. No significant differences were observed in the amounts of dynein 1b (Motor) or IFT-particle proteins between wild-type flagella and *tpg* flagella. (B) Immunofluorescence microscopy of WT, *tpg1*, and *tpg2-1* using anti–acetylated tubulin antibody and anti-IFT46 antibody. Signals for IFT46 were observed in the basal bodies and the flagella of WT as well as *tpg1* and *tpg2-1*. Bars, 10 μm. Kymographs (C), velocities (D), and frequencies (E) of anterograde IFT and retrograde IFT of WT, *tpg1*, and *tpg2-1* as determined by DIC microscopy. SDs for each measurement are shown as bars.

that facilitates premeiotic flagellar shortening. The delay in the flagellar shortening of dikaryons between *tpg1* × *tpg2-1* heterodikaryons presumably reflects the time that is required for reconstitution and recruitment of TTLL9-FAP234 complexes into the flagella, where they subsequently catalyze polyglutamylation.

Tubulin polyglutamylation accelerates tubulin depolymerization/turnover at the flagellar tip

In the steady-state flagellum, tubulin is continuously turning over at the flagellar tip as a consequence of a dynamic process involving the balanced assembly and disassembly of the axoneme (Marshall and Rosenbaum, 2001; Ishikawa and Marshall, 2011). All of the results described in the foregoing suggest that the reduced tubulin polyglutamylation in the *tpg* mutants increases the stability of the axoneme; if so, one would expect that tubulin polyglutamylation level would affect the tubulin turnover rate. Tubulin turnover can be assessed in *Chlamydomonas* zygotes by mating a gamete expressing α-tubulin having a C-terminal HA tag to one expressing untagged tubulin and then monitoring incorporation of the tagged tubulin into the tips of the flagella derived from the

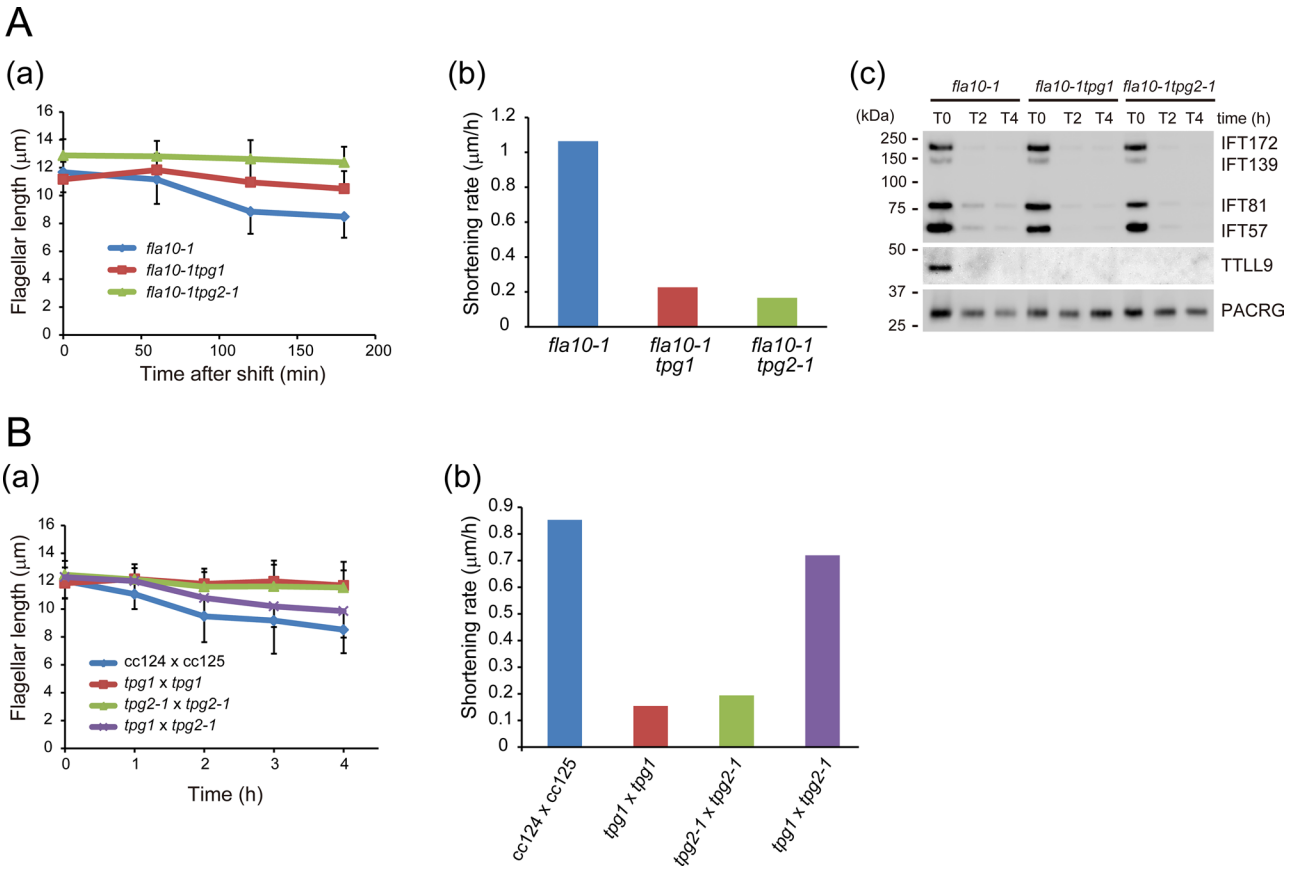

FIGURE 4: Tubulin polyglutamylation deficiency decelerates flagellar disassembly in IFT-inhibited cells and flagellar-resorbing zygotes. (A) (a) Change in flagellar length of *fla10-1* (a temperature-sensitive mutant of the anterograde IFT motor kinesin-2), *fla10-1tpg1*, and *fla10-1tpg2-1* upon temperature shift from 23 to 33°C (nonpermissive temperature). *fla10-1tpg1* and *fla10-1tpg2-1* flagella shortened more slowly than those of *fla10-1*. SDs for each measurement are shown as bars. There are statistically significant differences between *fla10* and *fla10tpg1* or between *fla10* and *fla10tpg2-1* after 120 min (*t* test, $p < 0.001$). (b) Flagellar shortening rate of *fla10-1*, *fla10-1tpg1*, and *fla10-1tpg2-1* at nonpermissive temperature. (c) Western blot of flagella from an experiment similar to that of A(a) probed with the indicated antibodies. IFT-particle proteins were rapidly depleted from flagella after the temperature shift. (B) (a) Flagellar shortening in quadriflagellated dikaryons from the following matings: wild type (CC124 × CC125), *tpg1* × *tpg1*, *tpg2-1* × *tpg2-1*, and *tpg1* × *tpg2-1*. Time 0 denotes when the mating was initiated. In contrast to wild-type dikaryons, *tpg1* and *tpg2-1* homodikaryons did not undergo flagellar shortening for at least 4 h. Of interest, after an ~1-h lag, *tpg1* × *tpg2-1* heterodikaryons were capable of undergoing flagellar shortening, presumably due to cytoplasmic complementation. (b) Flagellar shortening rate of quadriflagellated dikaryons. Because there is an ~1-h time lag before flagellar shortening is initiated in *tpg1* × *tpg2-1* dikaryons, we used data sets after 1 h for all dikaryons.

untagged gamete. Therefore, to determine the effect of polyglutamylation on tubulin turnover, we mated wild-type or *tpg2-1* gametes expressing tubulin-HA to wild-type or *tpg2-1* gametes expressing only untagged tubulin, respectively. As expected, flagella were slightly longer in the *tpg2-1* zygotes than in the wild-type zygotes (Figure 5B). In the wild-type zygotes, incorporation of tubulin-HA into the tips of the formerly untagged flagella was clearly observed by immunostaining of the HA tag (Figure 5, A and C), indicating that tubulin in this region is undergoing reversible polymerization and depolymerization. In contrast, tubulin-HA incorporation was greatly reduced in the *tpg2-1* background (Figure 5, A and C), indicating that tubulin polyglutamylation deficiency greatly lowers tubulin turnover at the flagellar tips. These results also suggest that the polyglutamylation-deficient axonemal microtubules are more stable than normal.

Tubulin polyglutamylation promotes flagellar elongation induced by lithium

Lithium is known to elongate *Chlamydomonas* flagella as well as primary cilia of mouse brain (Nakamura *et al.*, 1987; Miyoshi *et al.*, 2009). Although the precise mechanism is not known, experiments on *Chlamydomonas* flagella have suggested that lithium inhibits the activity of glycogen synthase kinase 3, which is involved in the regulation of flagellar length (Wilson and Lefebvre, 2004). We tested the effect of lithium on the flagella of *tpg1* and *tpg2* mutants. On the addition of 25 mM LiCl, the flagella of wild-type cells started to elongate from their original length of ~12 μm, reaching ~20 μm within 2 h (Figure 6Aa). However, in *tpg1*, *tpg2-1*, and *tpg2-3*, lithium-induced flagellar elongation was modest compared with that of wild type. Therefore lithium is less effective at inducing flagellar elongation in strains with a deficiency in axonemal polyglutamylation.

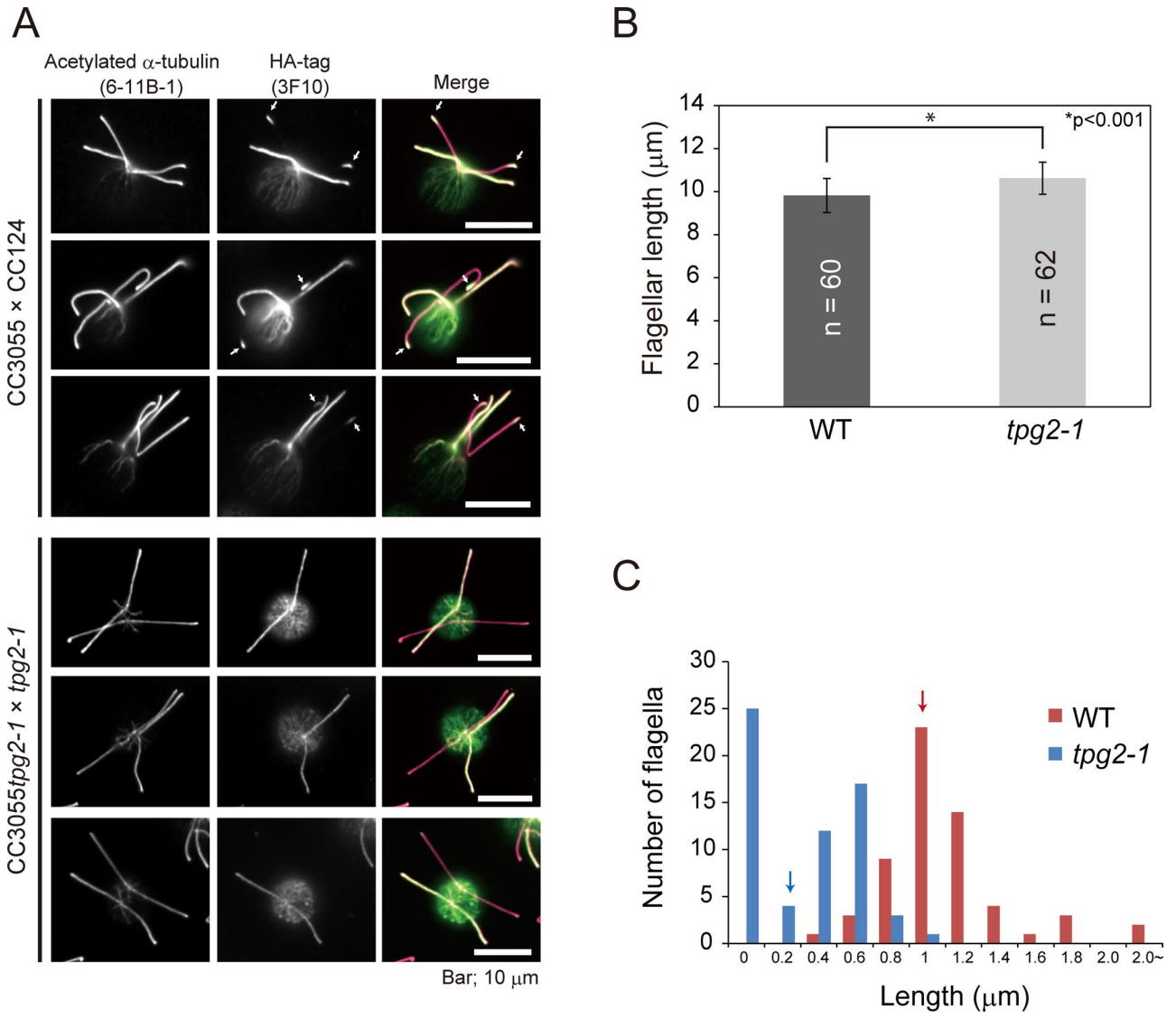

FIGURE 5: Tubulin polyglutamylation deficiency decreases tubulin turnover/depolymerization rate at the flagellar tip. (A) Immunofluorescence microscopy of dikaryons produced by mating gametes of wild type (CC124) with gametes of a strain (CC3055) expressing HA-tagged α-tubulin or by mating gametes of *tpg2-1* to those of CC3055*tpg2-1*. Cells were fixed and stained with anti–acetylated α-tubulin and anti–HA-tag antibodies 1.5 h after mating was initiated by mixing gametes together. In the dikaryon of CC124 × CC3055, incorporation of tubulin-HA at the flagellar tips was clearly observed (arrows). By comparison, in the dikaryon of *tpg2-1* × CC3055*tpg2-1*, the amount of tubulin-HA incorporation was greatly reduced. Bars, 10 μm. (B) Flagellar length of dikaryons. In both matings, only the flagella contributed by the gamete expressing tubulin-HA was measured. SD is shown as bars. The asterisk indicates a statistically significant differences (*t* test, $p < 0.001$). (C) Histograms showing the length of the tubulin-HA–labeled regions at the flagellar tips. The arrows indicate average length for each data set. Tubulin-HA incorporation into the flagellar tips was inhibited in *tpg2-1* dikaryons, indicating that the polyglutamylation deficiency decreases the tubulin turnover rate.

Lithium may be initiating an elongation mechanism that does not function normally in such strains.

Western blotting demonstrated that the amounts of IFT-particle proteins in both wild-type and *tpg1* flagella slightly increase after addition of lithium (Figure 6Ab). This result is consistent with the previous observation that lithium-induced flagellar elongation is associated with an increase in the amount of IFT172 and FLA10 in wild-type flagella (Wilson and Lefebvre, 2004). However, in the presence of tubulin polyglutamylation deficiency, this increase is not sufficient to support typical lithium-induced flagellar elongation. This highlights the importance of tubulin polyglutamylation for control of flagellar length.

tpg1 and *tpg2* mutants undergo normal flagellar shortening induced by sodium pyrophosphate

Sodium pyrophosphate (NaPPi) is a phosphatase inhibitor as well as calcium chelator that causes a rapid shortening of wild-type flagella (Lefebvre *et al.*, 1978; Quader *et al.*, 1978). IFT is not directly involved in this process, since the *fla10-1* mutant at nonpermissive temperature also rapidly shortens in NaPPi (Pan and Snell, 2005). To

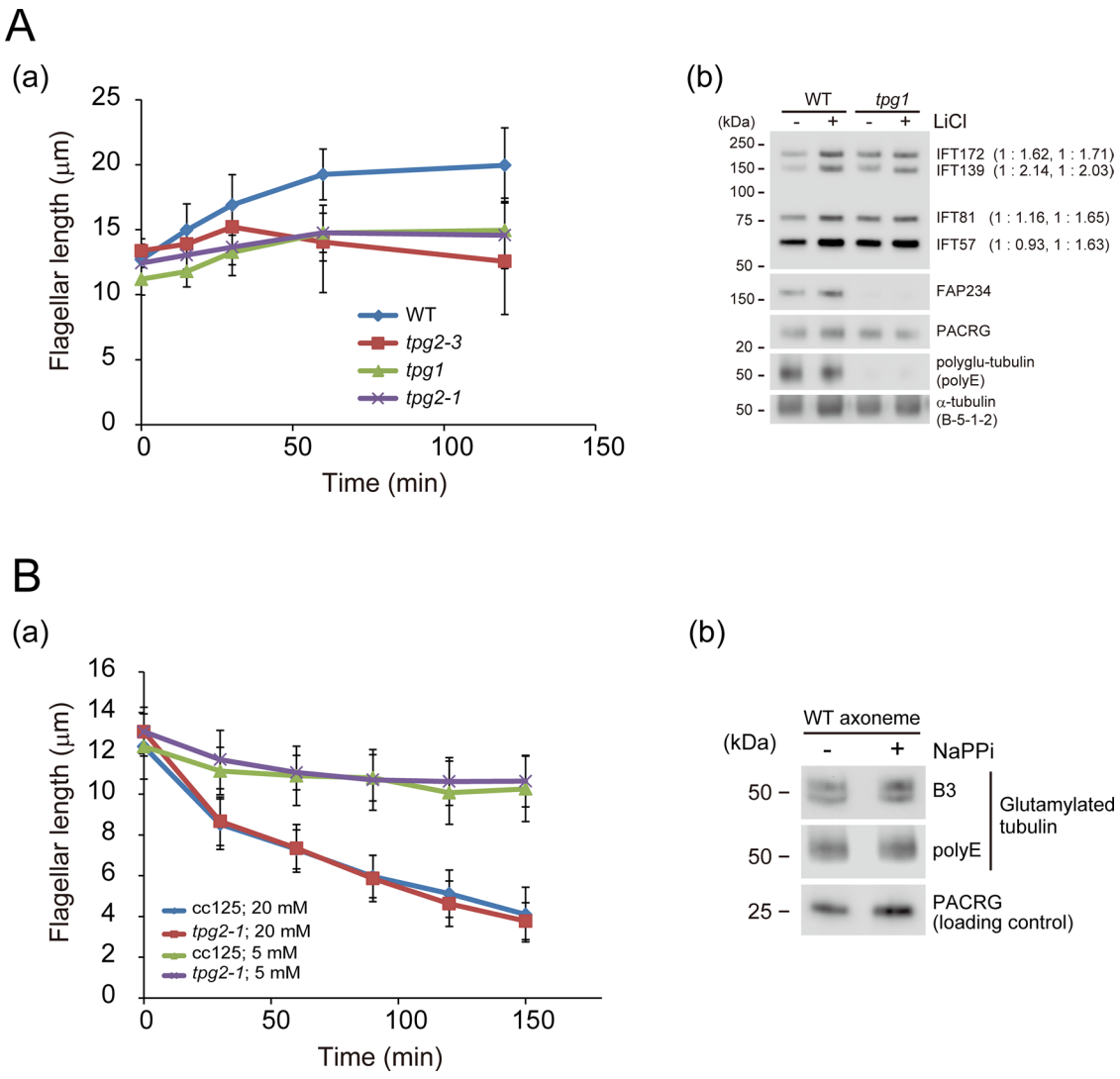

FIGURE 6: Effects of tubulin polyglutamylation deficiency under nonphysiological conditions. (A) (a) Flagellar elongation in WT, *tpg1*, *tpg2-1*, and *tpg2-3* treated with LiCl (25 mM). The *tpg* flagella did not elongate as much as the WT flagella. (b) Flagella of WT and *tpg1* cells were analyzed by Western blotting using antibodies to the indicated proteins. Flagella were isolated 60 min after LiCl addition. LiCl caused a slight increase in IFT proteins in the flagella of WT and *tpg1*. A similar result was previously shown for WT flagella by Wilson and Lefebvre (2004). (B) (a) NaPPi (5 and 20 mM)-induced flagellar shortening in WT (CC125) and *tpg2-1*. In this case, no differences were observed between the two strains. (b) Western blot of WT axonemes from cells treated with or without NaPPi (20 mM, 30 min) probed with the indicated antibodies.

see whether tubulin polyglutamylation deficiency also inhibits NaPPi-induced flagellar resorption, we added 5 and 20 mM NaPPi to cell cultures of wild type and *tpg2-1*. The time course of flagellar shortening in *tpg2-1* after the addition of NaPPi was identical to that of wild type (Figure 6Ba). In addition, the polyglutamylation level of wild-type axonemes did not change significantly after the addition of NaPPi (Figure 6Bb). These results demonstrate that the pathway of flagellar shortening induced by NaPPi differs from that involved in the TTLL9/FAP234 control of flagellar length.

DISCUSSION

In this study, we showed that the *ssh1* mutation, originally isolated as a mutation that promotes flagellar elongation in dynein-deficient strains having short flagella, is a new loss-of-function allele of *TPG2*, a gene necessary for normal polyglutamylation of axonemal tubulin. This finding caused us to consider why dynein-deficient strains have short flagella and why reduced polyglutamylation leads to flagellar elongation.

Flagellar shortening in mutants lacking outer doublet microtubule substructures likely results from outer doublet destabilization

We found that loss of either FAP234 or TTLL9, both of which are necessary for normal tubulin polyglutamylation, restored length to flagella deficient in a wide variety of axonemal substructures, including inner and outer dynein arms, the outer dynein arm docking complex, radial spokes, the N-DRC, and even the central pair of microtubules. Microtubule-associated proteins are known to stabilize microtubules and promote microtubule assembly (Drewes *et al.*, 1998), and it is likely that loss of the aforementioned outer doublet microtubule-associated structures destabilizes the outer doublets, leading to axonemal shortening. Consistent with this, the shortening

associated with loss of axonemal structures in *Chlamydomonas* is cumulative, with loss of multiple components having a greater effect on flagellar length than the absence of any one component alone (Figure 2 and Supplemental Figure S3). Reduced polyglutamylation probably restores flagellar length in these mutants by increasing outer doublet microtubule stability, a hypothesis supported by our observations on how changes in polyglutamylation level affect flagellar shortening and microtubule turnover (see the following section).

The *shortness* caused by loss of the central pair in *pf18* flagella likely occurs by a different mechanism, one that does not involve outer doublet destabilization (Lechtreck *et al*., 2013). Nevertheless, the flagellar elongation that results when *pf18* is combined with *tpg1* (Supplemental Figure S3D) may be caused by the same mechanism as the one that causes longer flagella when the *tpg* mutations are placed in an otherwise wild-type background—namely, reduced tubulin polyglutamylation resulting in outer doublet microtubules that are more stable than normal, leading to increased tubulin incorporation and flagellar lengthening.

The level of tubulin polyglutamylation is a determinant of flagellar microtubule stability

Our finding that the degree of flagellar shortening that occurred in a mutant lacking outer and inner dynein arms was dependent on the level of TTLL9 expression confirmed the role of polyglutamylation in flagellar length control. Further experiments supported the hypothesis that the changes in tubulin polyglutamylation level affected flagellar length through a mechanism involving stabilization of microtubules. First, we found that shortening of *fla10-1* flagella at restrictive temperature, a measure of the rate of axonemal microtubule disassembly, was reduced in the absence of TTLL9. Second, the time-dependent shortening of flagella in newly formed zygotes was severely reduced in the absence of TTLL9. Both results strongly suggest that the rate of axonemal microtubule disassembly is lowered when tubulin polyglutamylation is reduced. Third, the rate of tubulin turnover at the tip of the flagellum was decreased in the absence of TTLL9. This also is consistent with increased outer doublet stability in the polyglutamylation-deficient axonemes. Increased outer doublet stability would be expected ultimately to lead to longer flagella by tipping the microtubule assembly/disassembly balance toward assembly. However, length regulation is undoubtedly highly complex, involving interplay between, for example, tip-binding proteins that increase or decrease the rate of addition of tubulin subunits to the polymer (Slep and Vale, 2007) and regulatory kinases, such as LF4 and CNK2, that may be involved in a feedback mechanism between flagellar length and the rate of addition of tubulin subunits to the tip of the outer doublets (Hilton *et al*., 2013). Microtubule stability as a result of polyglutamylation level is likely to be just one of many factors contributing to length control.

Indeed, the complexity of flagellar length regulation is demonstrated by our observation that the flagellar elongation that is induced in wild-type cells by LiCl was greatly attenuated in cells with deficient tubulin polyglutamylation. This result also is consistent with microtubule stabilization and reduced tubulin turnover in the absence of TTLL9, although it is not clear why the large incorporation of additional tubulin subunits into the axoneme in the presence of LiCl was precluded. The results suggest that the mechanism by which flagellar elongation occurs in LiCl is not fully functional in the absence of normal tubulin polyglutamylation. Although LiCl has been believed to act on cilia via inhibition of glycogen synthase kinase 3 (Wilson and Lefebvre, 2004) or adenylate cyclase III (Ou *et al*., 2009), it recently was reported that, in mammalian cells, LiCl induces ciliary elongation by increasing the amount of acetylated α-tubulin in the cells (Nakakura *et al*., 2015); perhaps α-tubulin acetylation is not sufficient to promote axonemal elongation in the absence of normal tubulin polyglutamylation. The flagellar shortening that is induced by another nonphysiological condition—treatment with NaPPi—was not affected in the absence of TTLL9, suggesting that NaPPi-induced shortening occurs by a pathway unaffected by polyglutamylation levels.

Evidence for a role of tubulin polyglutamylation in the control of outer doublet stability also has come from studies in *C. elegans*, in which *increased* polyglutamylation led to progressive loss of the B-tubules in sensory cilia (O' Hagan *et al*., 2011), and in *Tetrahymena*, in which hyperglutamylation led to shorter cilia, also with broken or missing B-tubules (Wloga *et al*., 2010). In contrast, similar defects in the B-tubules were caused by TTLL6-knockdown mutations that *decrease* tubulin polyglutamylation in zebrafish cilia (Pathak *et al*., 2007, 2011). In our studies (Figure 1B), in the *Tetrahymena* studies, and possibly in the *C. elegans* studies, only long polyglutamate chains were affected; it may be that in the zebrafish studies, short polyglutamate side chains also were lost, leading to a different outcome.

Possible mechanism by which tubulin polyglutamylation affects microtubule disassembly

There are at least two possibilities that could account for the stabilization of polyglutamylation-deficient microtubules. One is that polyglutamylation changes the intrinsic properties of microtubules. Reduction of polyglutamylation may enhance the affinity between tubulin dimers or between protofilaments, generating more stable axonemal microtubules. This hypothesis could be tested in vitro using purified axonemal tubulin from *tpg* mutants.

A second possibility is that polyglutamylation changes the affinity between microtubules and microtubule-associated proteins such as microtubule-depolymerizing kinesins (Piao *et al*., 2009; Niwa *et al*., 2012; Wang *et al*., 2013), microtubule-elongating kinesins (Sardar *et al*., 2010), or microtubule plus end–binding proteins like EB1 (Pedersen *et al*., 2003; Shröder *et al*., 2007), with consequences for outer doublet microtubule stability and turnover.

A cautionary note on use of *ssh1* to suppress flagellar length

Finally, we point out that the *ssh1* mutation has an effect on the function of axonemal dynein. We previously demonstrated that tubulin polyglutamylation specifically influences the function of inner arm dynein and that the *tpg1* mutation increases the microtubule sliding velocity in axonemes lacking outer arm dynein (Kubo *et al*., 2010, 2012). Reduction of tubulin polyglutamylation apparently changes the overall function of dynein motors, probably by decreasing the binding affinity between axonemal microtubules and inner-arm dynein e (Kubo *et al*., 2012). Therefore, although *ssh1* is a useful tool for generating longer flagella from certain mutants, the present study indicates that researchers should use caution in interpreting biochemical and motility data from mutants carrying the *ssh1* mutation.

MATERIALS AND METHODS

Strains and cultures

Strains used in this study are listed in Supplemental Table S1. The mutant *ssh1* was kindly provided by Gianni Piperno (formerly Mount Sinai School of Medicine, New York, NY). Of the two *tpg2* isolates previously reported (Kubo *et al*., 2014), *tpg2-1* was predominantly used in this study. Cells were grown in M medium I (Sager and Granick, 1954) or TAP medium (Gorman and Levine, 1965).

Triple mutants (*pf28pf30tpg1*, *pf28pf30tpg2-1*, and *oda3ida1tpg2-1*) were produced by mating the following pairs using standard procedures (Harris, 2009): *pf28pf30* and *tpg1*, *pf28pf30* and *tpg2-1*, and *oda3ida1* and *tpg2-1*. Assuming that the mutants possessing defects in both outer arm dynein and axonemal tubulin polyglutamylation have phenotypes similar to *oda2tpg1* (Kubo *et al.*, 2010), the candidates for the triple mutants were selected from progenies based on their phenotypes of normal-length flagella with no motility. Finally, the strains harboring three mutations were determined by Western blotting of the isolated axonemes probed with anti-TTLL9, anti–polyglutamylated tubulin, anti-IC140, and anti-IC2 antibodies (Supplemental Figure S5).

Identification of *ssh1* mutation and transformation of the cell

The gene mutated in *ssh1* was determined by AFLP analysis (Kathir *et al.*, 2003) in combination with the *Chlamydomonas* genome database (genome.jgi-psf.org/Chlre4/Chlre4.home.html) and flagella proteome database (Pazour *et al.*, 2005). The primers used in this study are listed in Supplemental Table S2 of Kubo *et al*. (2014).

To generate *pf28pf30tpg1::TTLL9HA* strains, *pf28pf30tpg1* was cotransformed with a construct encoding TTLL9-HA (Kubo *et al.*, 2014) and the paromomycin resistance gene and selected on a TAP agar plate containing 10 μg/ml paromomycin (Sigma, St. Louis, MO). Expression of TTLL9-HA was confirmed by Western blotting using anti–HA-tag antibody (3F10).

Preparation of protein samples

Flagella and axonemes were isolated by the method of Witman *et al*. (1978). Whole-cell samples were prepared according to Fowkes and Mitchell (1998). Briefly, cytoplasmic proteins from whole cells were precipitated with methanol and chloroform and washed twice with methanol. The cytoplasmic proteins were solubilized in a solution containing 5 M urea, 2 M thiourea, and 0.05% Triton X-100.

SDS–PAGE and Western blotting

Proteins were separated by SDS–PAGE on 7.5 or 9% gels (Laemmli, 1970). The gels were either stained with Coomassie brilliant blue or processed for Western blotting. Primary antibodies used for Western blotting are listed in Supplemental Table S2. The signals were detected with anti-mouse, anti-rabbit, or anti-rat immunoglobulin G conjugated with horseradish peroxidase (Life Technologies, Carlsbad, CA) and chemiluminescent substrate (SuperSignal West Pico; Life Technologies).

Flagellar length measurement

Fully grown cells were mixed with 2% glutaraldehyde and observed using an inverted microscope. In most experiments, at least 30 cell images were collected, and flagellar lengths were measured using ImageJ (National Institutes of Health, Bethesda, MD). In calculating average flagellar length, we included only those cells with flagella. In some experiments, palmelloid cells were induced to grow flagella by treatment with autolysin prepared by the method of Craige *et al*. (2010).

Zygote production

Zygotes were generated by standard procedures (Harris, 2009). Briefly, cells of opposite mating types grown on TAP medium plates for 6–7 d were transferred to liquid M-N medium (M medium without nitrogen; Sager and Granick, 1954) and incubated for 3–5 h. Gametes of plus and minus mating types were mixed and incubated to produce zygotes.

Immunofluorescence microscopy

Indirect immunofluorescence microscopy was performed following Sanders and Salisbury (1995) and Craige *et al*. (2010). Cells attached to a coverslip were fixed with –20°C methanol for 15 min and incubated with the primary antibodies listed in Supplemental Table S2, followed by staining with the secondary antibodies conjugated with Alexa 488 and Alexa 594 (1:2000; Life Technologies). The specimens were mounted in Prolong Gold (Invitrogen) on a slide glass. The slides were observed with an Axioskop II plus (Carl Zeiss, Thornwood, NY) equipped with a 100× Plan-Apochromat 1.4 numerical aperture (NA) objective. Images were obtained with an AxioCam MRm camera (Carl Zeiss) and AxioVision software (Carl Zeiss).

Observation of IFT

Observation of IFT in live cells was carried out following Dentler (2005) and Craige *et al*. (2010). Flagella attached to the coverslip were observed with an inverted microscope (Ti-U; Nikon) equipped with a 1.4 NA oil-immersion condenser, a 60×/1.49 NA objective lens, a high-contrast DIC prism, and a green filter. A Lumen 220 lamp (Prior Scientific, Rockland, MA) was used as the light source. Images were captured at 30 frames/s with an iXon3 electron-multiplying charge-coupled device (CCD) camera (Andor Technology, Belfast, Northern Ireland) and analyzed by ImageJ to obtain the speeds and the frequencies of IFT-particle movement.

Assessment of flagellar motility

Swimming velocities of the mutants were measured by tracking images of swimming cells recorded using a dark-field microscope with a 40× objective and a CCD camera. Images were analyzed by ImageJ to acquire the swimming velocities.

ACKNOWLEDGMENTS

We thank Gianni Piperno (formerly Mount Sinai School of Medicine, New York, NY) and David R. Mitchell (State University of New York, Syracuse, NY) for providing strains. This study was supported by a Japan Society for the Promotion of Science Postdoctoral Fellowship (to T.K.), a Uehara Memorial Foundation Research Fellowship for Research Abroad (to T.K.), grants-in-aid from the Japan Society for Promotion of Science (23657046 and 24370079 to M.H. and 23570189 to R.K.), a National Institutes of Health grant (GM30626 to G.W.), and the Robert W. Booth Endowment at the University of Massachusetts Medical School (to G.W.).

REFERENCES

Berman SA, Wilson NF, Haas NA, Lefebvre PA (2003). A novel MAP kinase regulates flagellar length in *Chlamydomonas*. Curr Biol 13, 1145–1149.

Bradley BA, Quarmby LM (2005). A NIMA-related kinase, Cnk2p, regulates both flagellar length and cell size in *Chlamydomonas*. J Cell Sci 118, 3317–3326.

Brokaw CJ, Kamiya R (1987). Bending patterns of *Chlamydomonas* flagella: IV. Mutants with defects in inner and outer dynein arms indicate differences in dynein arm function. Cell Motil Cytoskeleton 8, 68–75.

Cao M, Li G, Pan J (2009). Regulation of cilia assembly, disassembly, and length by protein phosphorylation. Methods Cell Biol 94, 333–346.

Cavalier-Smith T (1974). Basal body and flagellar development during the vegetative cell cycle and the sexual cycle of *Chlamydomonas reinhardii*. J Cell Sci 16, 529–556.

Craige B, Tsao CC, Diener DR, Hou Y, Lechtreck KF, Rosenbaum JL, Witman GB (2010). CEP290 tethers flagellar transition zone microtubules to the membrane and regulates flagellar protein contents. J Cell Biol 190, 927–940.

Deane JA, Cole DG, Seeley ES, Diener DR, Rosenbaum JL (2001). Localization of intraflagellar transport protein IFT52 identifies basal body

transitional fibers as the docking site for IFT particles. Curr Biol 11, 1586–1590.
Dentler W (2005). Intraflagellar transport (IFT) during assembly and disassembly of *Chlamydomonas* flagella. J Cell Biol 170, 649–659.
Drewes G, Ebneth A, Mandelkow EM (1998). MAPs, MARKs and microtubule dynamics. Trends Biochem Sci 23, 307–311.
Fowkes ME, Mitchell DR (1998). The role of preassembled cytoplasmic complexes in assembly of flagellar dynein subunits. Mol Biol Cell 9, 2337–2347.
Freshour J, Yokoyama R, Mitchell DR (2007). *Chlamydomonas* flagellar outer row dynein assembly protein ODA7 interacts with both outer row and I1 inner row dyneins. J Biol Chem 282, 5404–5412.
Gorman DS, Levine RP (1965). Cytochrome f and plastocyanin: their sequence in the photosynthetic electron transport chain of *Chlamydomonas reinhardti*. Proc Natl Acad Sci USA 54, 1665–1669.
Harris E (2009). The *Chlamydomonas* Sourcebook, Vol. 1, 2nd ed., Amsterdam: Academic Press.
Heuser T, Raytchev M, Krell J, Porter ME, Nicastro D (2009). The dynein regulatory complex is the nexin link and a major regulatory node in cilia and flagella. J Cell Biol 187, 921–933.
Hilton LK, Gunawardane K, Kim JW, Schwarz MC, Quarmby LM (2013). The kinases LF4 and CNK2 control ciliary length by feedback regulation of assembly and disassembly rates. Curr Biol 23, 2208–2214.
Hou Y, Qin H, Follit JA, Pazour GJ, Rosenbaum JL, Witman GB (2007). Functional analysis of an individual IFT protein: IFT46 is required for transport of outer dynein arms into flagella. J Cell Biol 176, 653–665.
Huang B, Piperno G, Luck DJ (1979). Paralyzed flagella mutants of *Chlamydomonas reinhardtii* defective for axonemal doublet microtubule arms. J Biol Chem 254, 3091–3099.
Ishikawa H, Marshall WF (2011). Ciliogenesis: building the cell's antenna. Nat Rev Mol Cell Biol 12, 222–234.
Jarvik JW, Reinhart FD, Kuchka M, Adler SA (1984). Altered flagellar size-control in *sh-1* short-flagella mutants of *Chlamydomonas reinhardtii*. J Protozool 31, 199–204.
Kamiya R (1988). Mutations at twelve independent loci result in absence of outer dynein arms in *Chlamydomonas reinhardtii*. J Cell Biol 107, 2253–2258.
Kamiya R (2002). Functional diversity of axonemal dyneins as studied in *Chlamydomonas* mutants. Int Rev Cytol 219, 115–155.
Kamiya R, Kurimoto E, Muto E (1991). Two types of *Chlamydomonas* flagellar mutants missing different components of inner-arm dynein. J Cell Biol 112, 441–447.
Kathir P, LaVoie M, Brazelton WJ, Haas NA, Lefebvre PA, Silflow CD (2003). Molecular map of the *Chlamydomonas reinhardtii* nuclear geneme. Eukaryot Cell 2, 362–379.
Kato T, Kagami O, Yagi T, Kamiya R (1993). Isolation of two species of *Chlamydomonas reinhardtii* flagellar mutants, *ida5* and *ida6*, that lack a newly identified heavy chain of the inner dynein arm. Cell Struct Funct 18, 371–377.
Koutoulis A, Pazour GL, Wilkerson CG, Inaba K, Sheng H, Takada S, Witman GB (1997). The *Chlamydomonas reinhardtii ODA3* gene encodes a protein of the outer dynein arm docking complex. J Cell Biol 137, 1069–1080.
Kozminski KG, Beech PL, Rosenbaum JL (1995). The *Chlamydomonas* kinesin-like protein FLA10 is involved in motility associated with the flagellar membrane. J Cell Biol 131, 1517–1527.
Kozminski KG, Johnson KA, Forscher P, Rosenbaum JL (1993). A motility in the eukaryotic flagellum unrelated to flagellar beating. Proc Natl Acad Sci USA 90, 5519–5523.
Kubo T, Yagi T, Kamiya R (2012). Tubulin polyglutamylation regulates flagellar motility by controlling a specific inner-arm dynein that interacts with the dynein regulatory complex. Cytoskeleton 69, 1059–1068.
Kubo T, Yanagisawa HA, Liu Z, Shibuya R, Hirono M, Kamiya R (2014). A conserved flagella-associated protein in *Chlamydomonas*, FAP234, is essential for axonemal localization of tubulin polyglutamylase TTLL9. Mol Biol Cell 25, 107–117.
Kubo T, Yanagisawa HA, Yagi T, Hirono M, Kamiya R (2010). Tubulin polyglutamylation regulates axonemal motility by modulating activities of inner-arm dyneins. Curr Biol 20, 441–445.
Laemmli UK (1970). Cleavage of structural proteins during the assembly of the head of bacteriophage T4. Nature 227, 680–685.
Lechtreck KF, Geimer S (2000). Distribution of polyglutamylated tubulin in the flagellar apparatus of green flagellates. Cell Motil Cytoskeleton 47, 219–235.
Lechtreck KF, Gould TJ, Witman GB (2013). Flagellar central pair assembly in *Chlamydomonas reinhardtii*. Cilia 2, 15.
LeDizet M, Piperno G (1995). The light chain p28 associates with a subset of inner dynein arm heavy chains in *Chlamydomonas* axonemes. Mol Biol Cell 6, 697–711.
Lefebvre PA, Nordstrom SA, Moulder JE, Rosenbaum JL (1978). Flagellar elongation and shortening in *Chlamydomonas*. IV. Effects of flagellar detachment, regeneration, and resorption on the induction of protein synthesis. J Cell Biol 78, 8–27.
Marshall WF, Rosenbaum JL (2001). Intraflagellar transport balances continuous turnover of outer doublet microtubules: implications for flagellar length control. J Cell Biol 155, 405–414.
Mitchell DR, Rosenbaum JL (1985). A motile *Chlamydomonas* flagellar mutant that lacks outer dynein arms. J Cell Biol 100, 1228–1234.
Miyoshi K, Kasahara K, Miyazaki I, Asanuma M (2009). Lithium treatment elongates primary cilia in the mouse brain and in cultured cells. Biochem Biophys Res Commun 388, 757–762.
Nakakura T, Asano-Hoshino A, Suzuki T, Arisawa K, Tanaka H, Sekino Y, Kiuchi Y, Kawai K, Hagiwara H (2015). The elongation of primary cilia via the acetylation of α-tubulin by the treatment with lithium chloride in human fibroblast KD cells. Med Mol Morphol 48, 44–53.
Nakamura S, Takino H, Kojima MK (1987). Effect of lithium on flagellar length in *Chlamydomonas reinhardtii*. Cell Struct Funct 12, 369–374.
Niwa S, Nakajima K, Miki H, Minato Y, Wang D, Hirokawa N (2012). KIF19A is a microtubule-depolymerizing kinesin for ciliary length control. Dev Cell 23, 1167–1175.
O'Hagan R, Piasecki BP, Silva M, Phirke P, Nguyen KC, Hall DH, Swoboda P, Barr MM (2011). The tubulin deglutamylase CCPP-1 regulates the function and stability of sensory cilia in *C. elegans*. Curr Biol 21, 1685–1694.
Okada Y, Hirokawa N (2000). Mechanism of the single-headed processivity: diffusional anchoring between the K-loop of kinesin and the C-terminus of tubulin. Proc Natl Acad Sci USA 97, 640–645.
Omran H, Kobayashi D, Olbrich H, Tsukahara T, Loges NT, Hagiwara H, Zhang Q, Leblond G, O'Toole E, Hara C, *et al*. (2008). Ktu/PF13 is required for cytoplasmic pre-assembly of axonemal dyneins. Nature 456, 611–616.
Ou Y, Ruan Y, Cheng M, Moser JJ, Rattner JB, van der Hoorn FA (2009). Adenylate cyclase regulates elongation of mammalian primary cilia. Exp Cell Res 315, 2802–2817.
Pan J, Snell WJ (2005). *Chlamydomonas* shortens its flagella by activating axonemal disassembly, stimulating IFT particle trafficking, and blocking anterograde cargo loading. Dev Cell 9, 431–438.
Pathak N, Augstin CA, Drummond IA (2011). Tubulin tyrosine ligase-like genes *ttll3* and *ttll6* maintain zebrafish cilia structure and motility. J Biol Chem 286, 11685–11695.
Pathak N, Obara T, Mangos S, Liu Y, Drummond IA (2007). The zebrafish *fleer* gene encodes an essential regulator of cilia tubulin polyglutamylation. Mol Biol Cell 18, 4353–4364.
Pazour GJ, Agrin N, Leszyk J, Witman GB (2005). Proteomic analysis of a eukaryotic cilium. J Cell Biol 170, 103–113.
Pazour GJ, Dickert BL, Vucica Y, Seeley ES, Rosenbaum JL, Witman GB, Cole DG (2000). *Chlamydomonas* IFT88 and its mouse homologue, polycystic kidney disease gene tg737, are required for assembly of cilia and flagella. J Cell Biol 151, 709–718.
Pazour GJ, Dickert BL, Witman GB (1999). The DHC1b (DHC2) isoform of cytoplasmic dynein is required for flagellar assembly. J Cell Biol 144, 473–481.
Pedersen LB, Geimer S, Sloboda RD, Rosenbaum JL (2003). The microtubule plus end-tracking protein EB1 is localized to the flagellar tip and basal bodies in *Chlamydomonas reinhardtii*. Curr Biol 13, 1969–1974.
Piao T, Luo M, Wang L, Guo Y, Li D, Li P, Snell WJ, Pan J (2009). A microtubule depolymerizing kinesin functions during both flagellar disassembly and flagellar assembly in *Chlamydomonas*. Proc Natl Acad Sci USA 106, 4713–4718.
Piperno G, Mead K, Henderson S (1996). Inner dynein arms but not outer dynein arms require the activity of kinesin homologue protein KHP1(FLA10) to reach the distal part of flagella in *Chlamydomonas*. J Cell Biol 133, 371–379.
Piperno G, Mead K, Shestak W (1992). The inner dynein arms I2 interact with a "dynein regulatory complex" in *Chlamydomonas* flagella. J Cell Biol 118, 1455–1463.

Porter ME, Bower R, Knott JA, Byrd P, Dentler W (1999). Cytoplasmic dynein heavy chain 1b is required for flagellar assembly in *Chlamydomonas*. Mol Biol Cell 10, 693–712.
Qin H, Diener DR, Geimer S, Cole DG, Rosenbaum JL (2004). Intraflagellar transport (IFT) cargo: IFT transports flagellar precursors to the tips and turnover products to the cell body. J Cell Biol 164, 255–266.
Quader H, Cherniack J, Filner P (1978). Participation of calcium in flagellar shortening and regeneration in *Chlamydomonas reinhardii*. Exp Cell Res 113, 295–301.
Sager R, Granick S (1954). Nutritional control of sexuality in *Chlamydomonas reinhardi*. J Gen Physiol 37, 729–742.
Sanders MA, Salisbury JL (1995). Immunofluorescence microscopy of cilia and flagella. Methods Cell Biol 47, 163–169.
Sardar HS, Luczak VG, Lopez MM, Lister BC, Gilbert SP (2010). Mitotic kinesin CENP-E promotes microtubule plus-end elongation. Curr Biol 20, 1648–1653.
Shröder JM, Schneider L, Christensen ST, Pedersen LB (2007). EB1 is required for primary cilia assembly in fibroblasts. Curr Biol 17, 1134–1139.
Sirajuddin M, Rice LM, Vale RD (2014). Regulation of microtubule motors by tubulin isotypes and post-translational modifications. Nat Cell Biol 16, 335–344.
Slep KC, Vale RD (2007). Structural basis of microtubule plus end tracking by XMAP215, CLIP-170, and EB1. Mol Cell 27, 976–991.
Suryavanshi S, Eddé B, Fox LA, Guerrero S, Hard R, Hennessey T, Kabi A, Malison D, Pennock D, Sale WS, *et al.* (2010). Tubulin glutamylation regulates ciliary motility by altering inner dynein arm activity. Curr Biol 20, 435–440.
Takada S, Kamiya R (1994). Functional reconstitution of *Chlamydomonas* outer dynein arms from alpha-beta and gamma subunits: requirement of a third factor. J Cell Biol 126, 737–745.
Tam LF, Ranum PT, Lefebvre PA (2013). CDK5 regulates flagellar length and localizes to the base of the flagella in *Chlamydomonas*. Mol Biol Cell 24, 588–600.
Tam LW, Wilson NF, Lefebvre PA (2007). A CDK-related kinase regulates the length and assembly of flagella in *Chlamydomonas*. J Cell Biol 176, 819–829.
Tanner CA, Rompolas P, Patel-King RS, Gorbatyuk O, Wakabayashi K, Pazour GJ, King SM (2008). Three members of the LC8/DYNLL family are required for outer arm dynein motor function. Mol Biol Cell 19, 3724–3734.
Wang L, Piao T, Cao M, Qin T, Huang L, Deng H, Mao T, Pan J (2013). Flagellar regeneration requires cytoplasmic microtubule depolymerization and kinesin-13. J Cell Sci 126, 1531–1540.
Wilson NF, Lefebvre PA (2004). Regulation of flagellar assembly by glycogen synthase kinase 3 in *Chlamydomonas reinhardtii*. Eukaryot Cell 3, 1307–1319.
Wirschell M, Yang C, Yang P, Fox L, Yanagisawa HA, Kamiya R, Witman GB, Porter ME, Sale WS (2009). IC97 is a novel intermediate chain of I1 dynein that interacts with tubulin and regulates interdoublet sliding. Mol Biol Cell 20, 3044–3054.
Wirschell M, Zhao F, Yang C, Yang P, Diener D, Gaillard A, Rosenbaum JL, Sale WS (2008). Building a radial spoke: flagellar radial spoke protein 3 (RSP3) is a dimer. Cell Motil Cytoskeleton 65, 238–248.
Witman GB, Plummer J, Sander G (1978). *Chlamydomonas* flagellar mutants lacking radial spokes and central tubules. Structure, composition, and function of specific axonemal components. J Cell Biol 76, 729–747.
Wloga D, Dave D, Meagley J, Rogowski K, Jerka-Dziadosz M, Gaertig J (2010). Hyperglutamylation of tubulin can either stabilize or destabilize microtubules in the same cell. Eukaryot Cell 9, 184–193.
Wren KN, Craft JM, Tritschler D, Schauer A, Patel DK, Smith F, Porter ME, Kner P, Lechtreck KF (2013). A differential cargo-loading model of ciliary length regulation by IFT. Curr Biol 23, 2463–2471.
Yamamoto R, Hirono M, Kamiya R (2010). Discrete PIH proteins function in the cytoplasmic preassembly of different subsets of axonemal dyneins. J Cell Biol 190, 65–71.